Veterinary Immunology and Immunopathology 127 (2009) 277–285

Contents lists available at ScienceDirect

Veterinary Immunology and Immunopathology

journal homepage: www.elsevier.com/locate/vetimm

Research paper

Histology, immunohistochemistry and ultrastructure of the bovine palatine tonsil with special emphasis on reticular epithelium

Mitchell V. Palmer *, Tyler C. Thacker, W. Ray Waters

Bacterial Diseases of Livestock Research Unit, National Animal Disease Center, Agricultural Research Service, USDA, 2300 Dayton Avenue, Ames, IA 50010, USA

ARTICLE INFO

Article history:
Received 18 June 2008
Received in revised form 26 September 2008
Accepted 20 October 2008

Keywords:
Cattle
Histology
Lymphoid tissue
M-cell
Tonsil
Ultrastructure

ABSTRACT

The paired palatine tonsils, located at the junction of the nasopharynx and oropharynx, are ideally positioned to sample antigens entering through the nasal cavity or oral cavity. Entering antigens will first contact tonsilar epithelium. To better understand the cellular composition of this important epithelial layer, palatine tonsils were collected from six, 7-month-old calves and examined by light microscopy, immunohistochemistry and electron microscopy. Morphometric analysis showed that epithelium overlying lymphoid follicles (reticular epithelium) contained more B-cells, CD4+, CD8+, CD11c+, CD172a+ and γ/δ TCR+ cells than non-reticular epithelium, with B-cells, CD4+ cells and CD11c+ cells being most numerous. Scanning and transmission electron microscopy of reticular epithelium identified an interrupted basement membrane and vascular elements within the epithelium, as well as cells with characteristics morphologically consistent with cells identified as M-cells in other species. Bovine palatine tonsilar reticular epithelium contains key immune cells, as well as potential M-cell-like cells; elements essential for antigen uptake, antigen processing and initiation of immune responses.

Published by Elsevier B.V.

1. Introduction

Waldeyer's ring is composed of the nasopharyngeal tonsil (adenoid), paired tubal tonsils, paired palatine tonsils, lingual tonsils and tonsils of the soft palate (Nickel et al., 1979; Perry and Whyte, 1998). The palatine and nasopharyngeal tonsils, composed primarily of follicles, are known as follicular tonsils (Nickel et al., 1979). The mucosal layer of follicular tonsils contains numerous invaginations known as fossae or crypts that greatly expand surface area. In the human palatine tonsil it is estimated that the crypt epithelial surface area is 295 cm^2 (Perry and Whyte, 1998), while in sheep it is estimated that the epithelial surface area of the pharyngeal tonsil and paired palatine tonsils is 23.5 cm^2 and 7.14 cm^2, respectively (Casteleyn et al., 2008). Crypts are surrounded by nodular lymphoid tissue creating tonsilar lymphoid follicles (Nickel et al., 1979). In cattle, palatine tonsilar crypts open into a larger tonsilar sinus that communicates with the oral cavity. The paired palatine tonsils are located at the junction of the nasopharynx and oropharynx; ideally positioned to sample antigens entering through either the nasal or oral cavities.

Epithelium not associated with tonsilar lymphoid follicles (non-lymphoepithelial tonsilar epithelium or non-reticular epithelium) of the palatine tonsil is characterized as stratified non-keratinized or parakeratinized epithelium. Within this epithelium there are rare non-epithelial cells or vascular structures. In contrast, epithelium overlying lymphoid follicles (lymphoepithelium, follicle-associated epithelium, or reticular epithelium) (Perry and Whyte, 1998), is characterized by epithelial cells altered in shape and cellular content, infiltrative non-epithelial cells (lymphoid cells, macrophages and dendritic

* Corresponding author at: National Animal Disease Center, 2300 Dayton Avenue, Ames, IA 50010, United States. Tel.: +1 515 663 7474; fax: +1 515 663 7458.
E-mail address: mitchell.palmer@ars.usda.gov (M.V. Palmer).

0165-2427/$ – see front matter. Published by Elsevier B.V.
doi:10.1016/j.vetimm.2008.10.336

cells), intraepithelial vasculature, and a disrupted underlying basement membrane (Perry and Whyte, 1998). Reticular epithelium provides a venue for intimate contact between antigens, specialized epithelial cells, intraepithelial lymphocytes and antigen presenting cells, with subsequent antigen uptake and transport. Reticular epithelium in tonsils of some species also contains specialized epithelial cells (M-cells) that allow for selective sampling through endocytosis and transport of luminal antigens with exocytosis to immune cells within or below the mucosal layer. M-cells have been identified in bovine nasopharyngeal tonsils (Schuh and Oliphant, 1992), but not bovine palatine tonsils.

A detailed understanding of the bovine tonsil is important as it represents the first line of defense against foreign antigens entering by either the respiratory or digestive routes. Bovine palatine tonsils play a role in important diseases such as bovine viral diarrhea (Liebler-Tenorio et al., 1997), *Mannheimia haemolytica* induced pneumonia (Briggs et al., 1998), bovine tuberculosis (Cassidy et al., 1999), and bovine spongiform encephalopathy (Wells et al., 2005). The importance of lymphoepithelium in the pathogenesis of ruminant diseases such as paratuberculosis and tuberculosis has been reviewed (Lugton, 1999). Additionally, the palatine tonsil has been used as a route of exposure in models of tuberculosis in cattle and deer species (Griffin et al., 2006; Palmer et al., 1999a; Palmer et al., 1999b). Detailed studies of bovine tonsilar reticular epithelium have been limited to the nasopharyngeal tonsil (Schuh and Oliphant, 1992). Previous studies have contained limited descriptions of T-cells within the palatine and nasopharyngeal tonsilar reticular epithelium (Rebelatto et al., 2000). The objective of the current study was to characterize the cell type, distribution, morphology and ultrastructure of palatine tonsilar reticular epithelium, with special emphasis on the distribution of important lymphocyte subsets and presence of cells morphologically similar to M-cells.

2. Materials and methods

2.1. Animals

Six, 7-month-old, healthy Holstein steers were humanely euthanized and palatine tonsils collected and preserved both by snap-freezing in liquid nitrogen-cooled isopentane as well as by immersion in 10% neutral buffered formalin. Formalin-fixed tissues were further processed by routine paraffin-embedment techniques, cut in 5 μm sections, stained with hematoxylin and eosin (HE) or periodic acid Schiff stain (PAS) and examined by light microscopy.

2.2. Immunohistochemistry and morphometry

Frozen sections of palatine tonsil were cut by cryostat in 6 μm sections and processed for immunohistochemistry using primary antibodies to the cell markers B-B7, CD4, CD8, γ/δ T cell receptor (TCR), CD172a, CD11c, CD68, and CD14 (Table 1) as described previously (Frink et al., 2002; Kunkle et al., 1995) using HistoMark Biotin Streptavidin-HRP system (Kirkegaard and Perry, Gaithersburg, MD, USA) and 3,3′ diaminobenzidine-nickel (DAB-Ni peroxidase substrate, Vector Laboratories, Burlingame, CA, USA) as a peroxidase substrate. Non-specific protein binding was blocked using normal goat serum and endogenous peroxidase activity was quenched using 0.3% H_2O_2 in methanol prior to application of the primary antibody. Digital images of sections from all palatine tonsils were obtained with a light microscope (Nikon Eclipse E800; Nikon Co., Tokyo, Japan) and digital camera (Spot RT, Diagnostic Instruments Inc., Sterling Heights, MI, USA).

Table 1
Primary/secondary antibodies, suppliers and conditions used in immunohistochemical identification of cell markers.

	Cellular expression	Isotype	Supplier	Catalog no.	Dilution	Incubation time	Temperature
Primary antibody							
CD4	T_h	IgG2a	VMRD	ILA11	1:50	3 h	RT
CD8	T_c	IgM	VMRD	BAQ11A	1:500	3 h	RT
Gamma/delta TCR	γ/δ T cells	IgG2b	VMRD	GB21A	1:10,000	3 h	RT
CD172a	Mono, gran	IgG1	VMRD	DH59B	1:500	3 h	RT
CD11c	Mono, mac, NK	IgM	VMRD	BAQ153A	1:1000	3 h	RT
B-B7	B cells	IgG1	VMRD	GB25A	1:500	3 h	RT
CD14	Mono, mac	IgG1	VMRD	CAM36A	1:500	3 h	RT
CD68	Mono, mac	IgG1	Dako	M0718	1:500	3 h	RT
Secondary antibody							
Biotinylated goat anti-mouse IgM			Southern Biotech	1020-08	1:200	30 min	RT
Biotinylated goat anti-mouse IgG (H&L)			Kirkegaard and Perry	71-00-29	RTU	30 min	RT
Biotinylated goat anti-mouse IgM			Kirkegaard and Perry	01-18-03	1:200	30 min	RT
Immunofluorescence							
Alexa Fluor 488 goat anti-mouse IgG (H&L)			Molecular Probes	A-11029	1:800	30 min	RT
Alexa Fluor 488 goat anti-mouse IgM			Molecular Probes	A-21042	1:800	30 min	RT
Alexa Fluor 488 goat anti-mouse IgG1			Molecular Probes	A-21121	1:800	30 min	RT
Alexa Fluor 594 goat anti-mouse IgG (H&L)			Molecular Probes	A-11032	1:800	30 min	RT

RT, room temperature; RTU, ready to use, no dilution required; T_h, T helper lymphocyte; T_c, cytotoxic T lymphocyte; Mono, monocytes; Mac, macrophage; NK, natural killer cells; TCR, T cell receptor.

Images were analyzed using Image Pro-Plus (Media Cybernetics, Silver Springs, MD, USA). Ten random regions of reticular epithelium and 10 random regions of non-reticular epithelium were evaluated from each animal. Using image analysis software the area of epithelium was measured as well as the number of stained cells within the measured region of epithelium. The number of cells per unit area was then calculated. Distances were calibrated for each microscope objective using image analysis software and a standard micrometer bar.

Additionally samples of frozen tissue were processed for single or dual labeling immunofluorescence, using primary antibodies to CD11c, CD14 and CD172a and Alexa Fluor (Molecular Probes, Eugene, OR, USA) conjugated secondary antibodies (Table 1). To improve cell visibility, fluorescently labeled sections were coverslipped using mounting media with DAPI (Vectasheild mounting media with DAPI, Vector Laboratories). Fluorescent images were analyzed using the above Nikon microscope equipped with the VFM Epi-fluorescent attachment with xenon lamp (Nikon, Co.).

2.3. Electron microscopy

Samples for transmission electron microscopy (TEM) were immersed in 2.5% glutaraldehyde in 0.1 M cacodylate buffer at 4 °C. After 2 h fixation, tissue samples were rinsed in cacodylate buffer, postfixed in 1% osmium tetroxide, dehydrated in alcohols, cleared in propylene oxide, and embedded in epoxy resin. Sections of tonsil were cut at 1 μm, stained with toluidine blue, and examined by light microscopy. Ultrathin sections of appropriate areas were cut, stained with uranyl acetate and lead citrate, and examined with a FEI Tecnai 12 Biotwin (FEI company, Hillsboro, OR) transmission electron microscope. Samples for scanning electron microscopy (SEM) were fixed as described above for TEM, rinsed in cacodylate buffer, postfixed in 1% osmium tetroxide, dehydrated in alcohols, critical point dried, mounted on stubs and coated with gold in a sputter-coater. Samples were examined on JEOL 5800LV scanning electron microscope.

2.4. Statistical analysis

Mean values for cell density (cells/1000 μm^2) of cells immunoreactive for various surface markers by immunohistochemistry were compared using an unpaired Student's *t*-test with Welch's correction (GraphPad Prism, GraphPad Software, San Diego, CA). A p-value <0.05 was considered significant.

3. Results

3.1. Histology and ultrastructure

Epithelium of the palatine tonsilar crypts ranged from a continuous layer of non-keratinized stratified squamous epithelium (non-reticular epithelium) to areas of epithelium overlying lymphoid follicles which were disrupted by the infiltration of numerous non-epithelial mononuclear cells extending from the lymphoid follicle through the basement membrane effacing normal epithelial architecture (reticular epithelium). Reticular epithelium consisted of epithelial cells separated by wide intercellular spaces forming pockets containing many lymphocytes and lesser numbers of macrophages, plasma cells, neutrophils and cells morphologically compatible with dendritic cells (Fig. 1A). In some regions of reticular epithelium, non-epithelial cell infiltrates extended superficially to the crypt lumen. In these regions the most apical lymphoid cells communicated freely with the lumen or were separated from the lumen by an attenuated cell layer often representing the long cytoplasmic extension of a single cell (as thin as 0.1 μm) (Fig. 1B) Some cytoplasmic extensions spanned up to 50 μm across the luminal surface. Cells forming the luminal border of such pockets were less electron dense than surrounding cells, with a single elongate to angular nucleus, moderate numbers of cytoplasmic microvesicles (0.1–0.4 μm diameter), multivesicular bodies (up to 1.5 μm diameter), endoplasmic reticulum, polyribosomes, mitochondria, irregularly arranged microfilaments (8 nm diameter), and variable numbers of short irregular microvilli (0.1–0.3 μm in length) on the luminal surface (Fig. 1C). These cells often formed desmosomal attachments with surrounding cells of similar morphology or morphology consistent with squamous epithelial cells.

Periodic acid Schiff stained sections as well as electron microscopic imaging demonstrated an intact basement membrane in regions of non-reticular epithelium; however, a highly interrupted and discontinuous basement membrane was present in regions of reticular epithelium (Fig. 2). Lymphocytes and macrophages were numerous in regions of discontinuous basement membrane, presumably migrating from subjacent lymphoid structures to the reticular epithelium. Small blood vessels were seen within reticular epithelium lined by plump rounded epithelial cells (Fig. 3).

Examination of the palatine tonsil by SEM revealed an epithelial surface formed mostly by flat, angular squamous cells. Intermittently other cells, smaller than squamous cells, were found on the epithelial surface. These cells were round to oval and covered by closely packed, knob-like, microvilli (Fig. 4A). These cells were demarcated from surrounding cells by a shallow furrow. Microvillus covered cells were found singly and other times as multiple cells connected by microvillus covered extensions forming a lattice work around squamous cells. Also evident were regions of squamous epithelium disrupted by complete loss of surface cells leaving the underlying non-epithelial cells exposed. These areas likely corresponded to regions seen by light microscopy of reticular epithelium where leukocytes extended through the entire epithelial layer to the crypt lumen (Fig. 4B).

3.2. Immunohistochemistry

Labeling for various surface markers demonstrated reticular epithelium containing moderate to large numbers of CD4+, B-B7+, γ/δ TCR+, CD11c+, CD14+ and CD68+ cells and low numbers of CD8+ and CD172a+ cells. Morphometric analysis revealed differences between reticular and

non-reticular epithelium of greatest magnitude for CD4+, B-B7+ and CD11c+ cells (Fig. 5), although reticular epithelium also contained significantly more γ/δ TCR+, CD172a+ cells than did non-reticular epithelium. In contrast, reticular epithelium contained fewer CD8+ cells than non-reticular epithelium. Cells immunopositive for the above surface antigens were generally scattered in varying numbers within all levels of reticular epithelium (Fig. 6). In slight contrast, γ/δ TCR+ cells, while present in low to moderate numbers throughout the epithelial layer, were most numerous in the basal layer of reticular epithelium (Fig. 7).

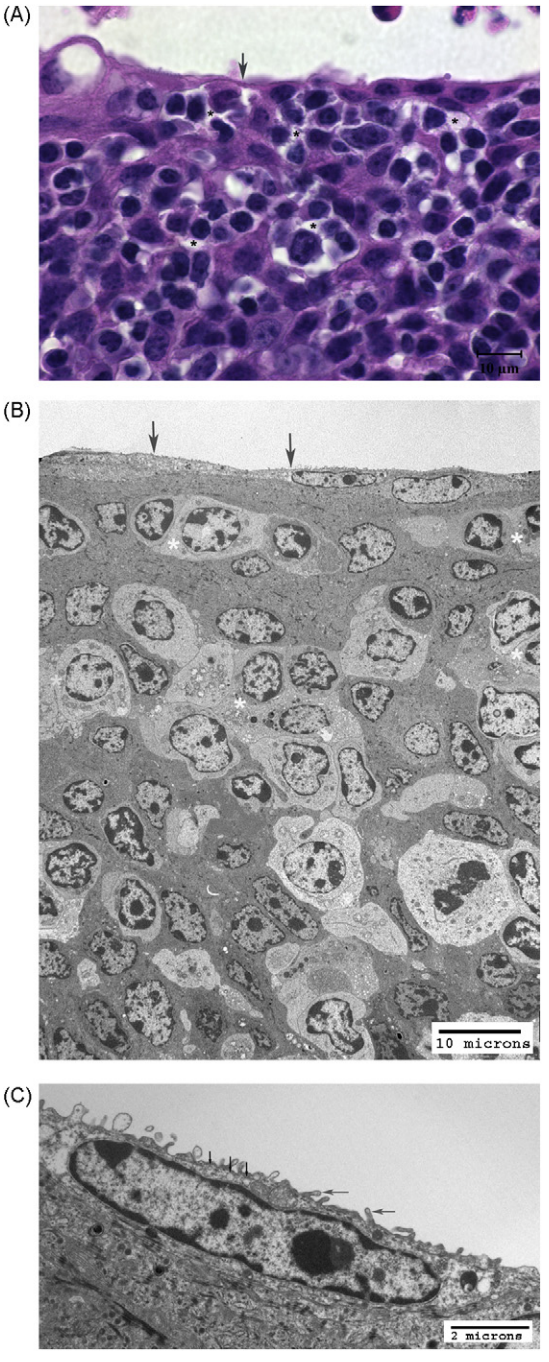

Fig. 1. Section of palatine tonsil from a 7-month-old steer. (A) Note reticular epithelium characterized by infiltrates of lymphocytes and other non-epithelial cells. Flattened and angular cells form pockets (asterisks) that contain non-epithelial cells. In some cases non-epithelial cells are separated from the crypt lumen only by a thin cytoplasmic process (arrow). H/E. Bar = 10 μm. (B) Electron micrograph of palatine tonsil showing pockets (asterisks) within reticular epithelium, the luminal surface of which is covered by flattened electron lucent cells (arrows). (C) Higher magnification of flattened cell with elongate nucleus, intracytoplasmic vesicles (small arrows) and numerous microvilli (large arrows). Bar = 2 μm.

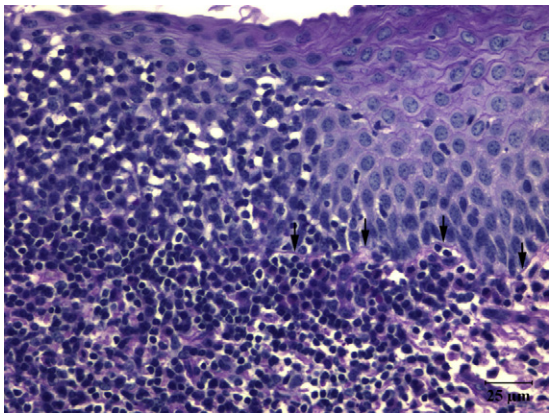

Fig. 2. Section of palatine tonsil from a 7-month-old steer. Junction of reticular and non-reticular epithelium demonstrates intact PAS positive basement membrane of non-reticular epithelium (arrows) and interrupted basement membrane of reticular epithelium (left half of image) and numerous infiltrative mononuclear non-epithelial cells. PAS. Bar = 25 μm.

Low numbers of round to stellate cells within the reticular epithelium stained positive for CD68 (Fig. 8A), a marker that has been associated with macrophages. In contrast, numerous cells within the reticular epithelium including cells with squamous morphology stained positive for the marker CD14 (Fig. 8B), also associated with macrophages (Fig. 8). Interestingly, CD14 staining of squamous cells was more pronounced in reticular epithelium compared to non-reticular epithelium (Fig. 8C). The markers CD172a and CD11c have been previously asso-

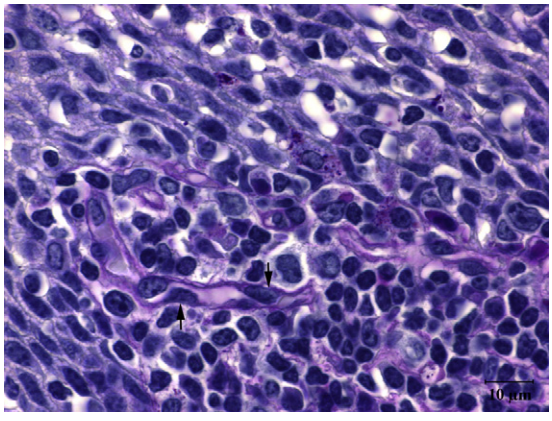

Fig. 3. Section of palatine tonsil from a 7-month-old steer. Within reticular epithelium are small caliber blood vessels lined by plump endothelial cells (arrows). PAS. Bar = 10 μm.

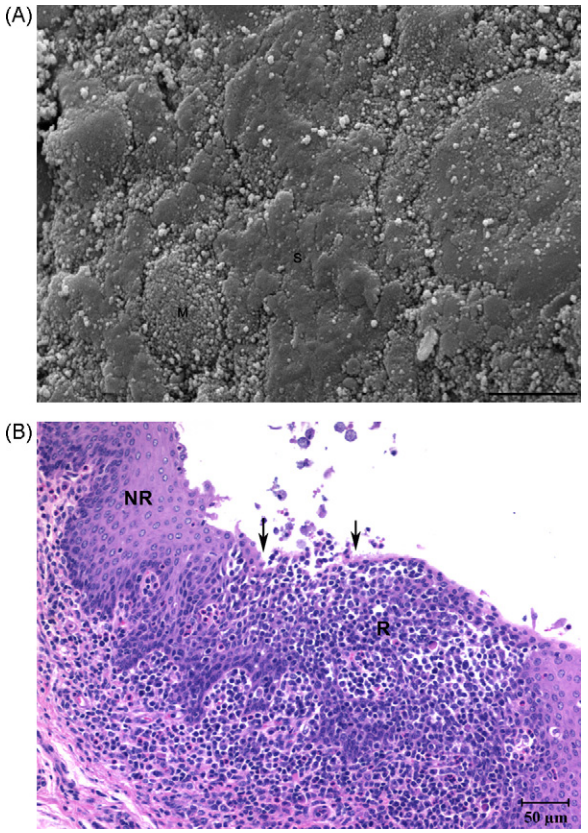

Fig. 4. Section of palatine tonsil from a 7-month-old steer. (A) Scanning electron micrograph reveals an epithelial surface mostly formed by flat, angular squamous cells (S). Intermittently other smaller cells covered by closely packed, knob-like microvilli are present (M). These cells are demarcated from surrounding cells by a shallow furrow. Microvillus covered cells are found singly or as multiple cells connected by microvillus covered extensions forming a lattice work around squamous cells. Bar = 2.5 μm. (B) Section of palatine tonsil at junction of reticular (R) and non-reticular (NR) epithelium. Note disrupted epithelial surface (between arrows) and lymphoid cells extending to crypt lumen. HE. Bar = 50 μm.

ciated with dendritic cells (Miyazawa et al., 2006). Within reticular epithelium, more cells stained positive for CD11c than CD172a; however, double labeling revealed that many cells staining for CD172a also stained positive for CD11c (Fig. 9A and B)). CD172a+ cells occasionally were arranged in clusters within reticular epithelium (Fig. 9C). Dual labeling using antibodies to CD172a and CD14 or CD11c and CD14 revealed cells within the reticular epithelium that stained for CD172a, CD11c and CD14 singly as well as both CD172a and CD14 or CD11c and CD14 (data not shown).

4. Discussion

The intestinal Peyer's patches represent the epitome of follicle-associated epithelium where reticular epithelium is composed of M-cells, lymphoid cells and normal epithelium. Luminal antigens, including microbes, are endocytosed and transported through M-cells and discharged into the intercellular space where dendritic cells, macrophages, T and B-lymphocytes, plasma cells and neutrophils are found. Luminal antigens are then transported by lymphoid cells or dendritic cells to the underlying lymphoid follicle for antigen presentation and initiation of an immune response. Other characteristics of lymphoepithelium include disrupted basement membrane, desquamation of upper epithelial layers, and infiltration of small intraepithelial blood vessels (Perry, 1994).

Histology and ultrastructure of bovine palatine and nasopharyngeal tonsils has been said to be similar to humans (Rebelatto et al., 2000). Most studies of the bovine palatine tonsils have described the tonsil as a whole and not focused specifically on the epithelium (Cocquyt et al., 2007, 2008; Manesse et al., 1998; Rebelatto et al., 2000; Velinova et al., 2001). The present study demonstrates that bovine palatine tonsilar reticular epithelium has many of the same characteristics of reticular epithelium in other anatomic locations such as intestinal Peyer's patches. Similar to findings in other species, bovine palatine tonsilar reticular epithelium contains large numbers of B-B7+ B-cells and CD4+ T-cells (Gebert and Pabst, 1999). Moreover, proportions of key immune cells such as B-cells, CD4+, CD8+ and γ/δ TCR+ T-cells were found to be similar in palatine tonsilar reticular epithelium to that described for bovine Peyer's patches and follicle-associated epithelium of ovine jejunum (Press et al., 1991), and is in agreement with other studies of the bovine palatine tonsil as a whole (Rebelatto et al., 2000). Additionally, the present study demonstrates that bovine palatine tonsilar reticular epithelium is characterized by an interrupted basement membrane and intraepithelial vasculature, characteristics of reticular epithelium in other tissues.

CD172a and CD11c have been demonstrated on a subset of bovine dendritic cells (Brooke et al., 1998; Renjifo et al., 1997), although macrophages may also express CD172a and CD11c, while some T-cells and B-cells may also express CD11c (Miyazawa et al., 2006). Bovine dendritic cells in peripheral blood are positive for both CD11c and CD172a expression, as are cells within the bovine thymus postulated to be dendritic cells of myeloid lineage (Miyazawa et al., 2006). In the present study, although the reticular epithelium contained greater numbers of CD11c+ cells compared to CD172a+ cells, dual labeling identified cells that expressed both markers, similar to putative dendritic cells in the bovine thymus (Miyazawa et al., 2006).

CD172a, also known as signal regulatory protein (SIRP) α, macrophage fusion receptor, or SHPS-1 is a transmembrane regulatory protein expressed primarily by myeloid cells (i.e., macrophages, monocytes, dendritic cells, granulocytes, myeloid progenitors), hematopoietic stem cells, and neurons (Barclay and Brown, 2006; van Beek et al., 2005). CD172a is essential for leukocyte trafficking through functional binding to the cell-associated ligand, CD47 (Liu et al., 2002; Vignery, 2005; Zen and Parkos, 2003). A population of cells of myeloid origin, with morphologic characteristics of monocytes, has been identified in both bovine spleen and peripheral blood. These cells express CD172a, CD11c and CD14, and have

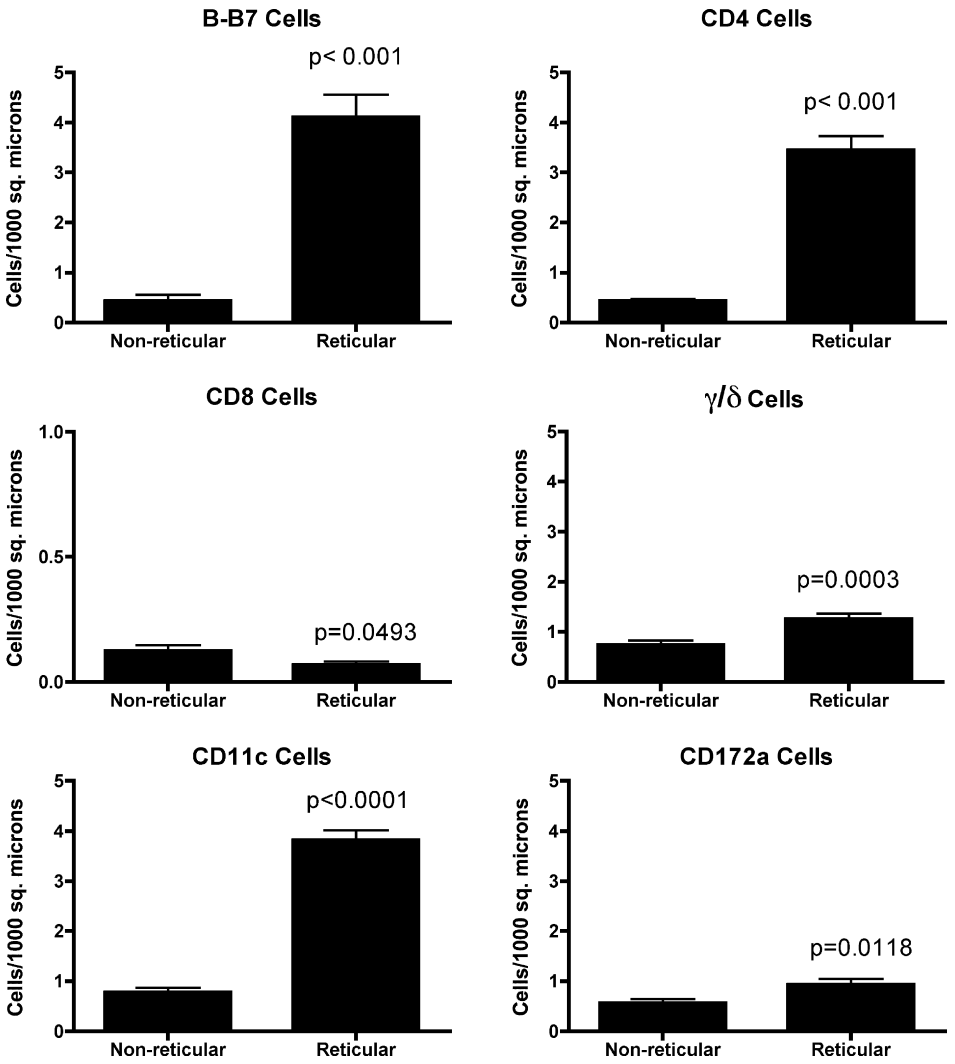

Fig. 5. Density (cells/1000 μm^2) of cells positive for various surface markers by immunohistochemistry. Data represent means ± S.E. from 10 random fields of reticular epithelium and 10 random fields of non-reticular epithelium from six 7-month-old steers.

been shown to produce nitric oxide in response to stimulation with heat killed *Mycobacterium bovis* BCG or *Babesia bovis* merozoites (Bastos et al., 2007).

CD14 and CD68 are both associated with macrophages; however, in the current study immunolabeling for these two markers yielded dissimilar patterns of expression. Although CD68 labeling was seen among scattered cells within the follicle, interfollicular regions, and epithelium, as would be expected of macrophages, CD14 expression was largely limited to polygonal or flattened cells of the reticular epithelium with little or no labeling of cells within the non-reticular epithelium. Distinct staining patterns for these two markers is not unexpected. CD68 is a glycoprotein associated with lysosomes in macrophages, myeloid cells and some neoplastic mononuclear cells and has previously been shown to label bovine macrophages including those found in tonsilar lymphoid follicles (Ackermann et al., 1994). In contrast, CD14 is a receptor for bacterial envelope constituents such as LPS (Pugin et al., 1994). Given the constant exposure of tonsilar epithelium to bacteria, labeling of cells within the reticular epithelium may represent expression of CD14 in response to exposure to bacterial constituents.

The presence of increased numbers of γ/δ TCR+ cells in palatine tonsilar reticular epithelium in the present study is consistent with previously held beliefs that γ/δ TCR+ cells localize preferentially to mucosal tissues and skin serving as a first line of defense (Hein and Mackay, 1991). In contrast to the present study, previous work with bovine tonsils demonstrated many CD8+ and γ/δ TCR+, and few CD4+ cells in tonsilar epithelium (Manesse et al., 1998). A separate study in adult cattle, showed >50% of all CD2+ cells to be CD8+ in the nasopharyngeal tonsilar epithelium (Schuh and Oliphant, 1992). The authors hypothesize that increased numbers of CD8+ T-cells in the tonsilar epithelium suggests a role for such cells that could include destruction of cells that have bound or ingested antigens (Manesse et al., 1998). A possible explanation for the

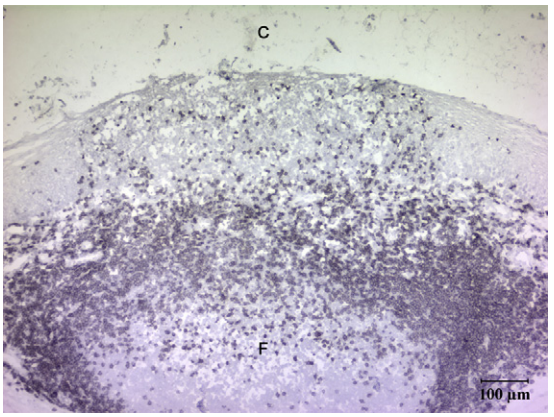

Fig. 6. Section of palatine tonsil from a 7-month-old steer. Labeling for CD4+ cells reveals immunoreactive cells extending from the follicle (F) superficially through the reticular epithelium. Many immunoreactive cells are found within pockets separated from the crypt lumen (C) by thin cytoplasmic extensions of non-immunoreactive cells. DAB-Ni, Harris hematoxylin counterstain. Bar = 100 μm.

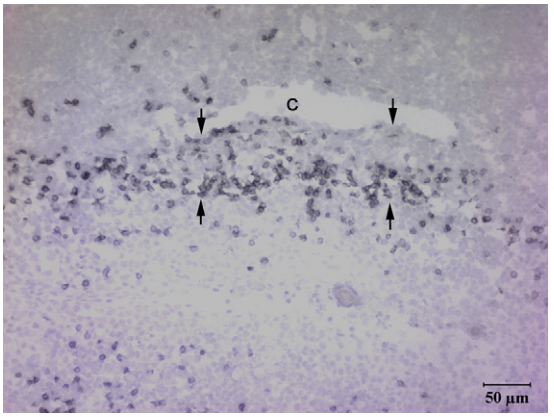

Fig. 7. Section of palatine tonsil from a 7-month-old steer. Labeling for γ/δ TCR+ cells reveals immunoreactive cells scattered within reticular epithelium (between arrows), but also along the basal region of the reticular epithelial layer. C: crypt lumen. DAB-Ni, Harris hematoxylin counterstain. Bar = 50 μm.

discrepancies between these studies may be different states of activation based on different antigen exposure in calves from the two studies, different ages of calves, or the focus on different tonsils, nasopharyngeal versus palatine. Alternatively, the present study and those by Manesse et al. and Schuh and Oliphant all used different antibodies to the CD8 surface marker to identify CD8+ cells. It is possible that each of the three antibodies labeled a different subset of CD8+ cells.

Typically, M-cells have characteristic short microvilli or microfolds on their luminal surface, lack cilia and mucus containing vesicles. Ultrastructural descriptions of M-cells include characteristics such as large euchromatic nuclei, prominent nucleoli, fine cytoplasmic filaments, and endocytic vesicles (Knop and Knop, 2005). Microvillus surface projections, the structural feature from which M-cells derive their name, usually differ from that of surrounding cells; however, their exact morphology varies

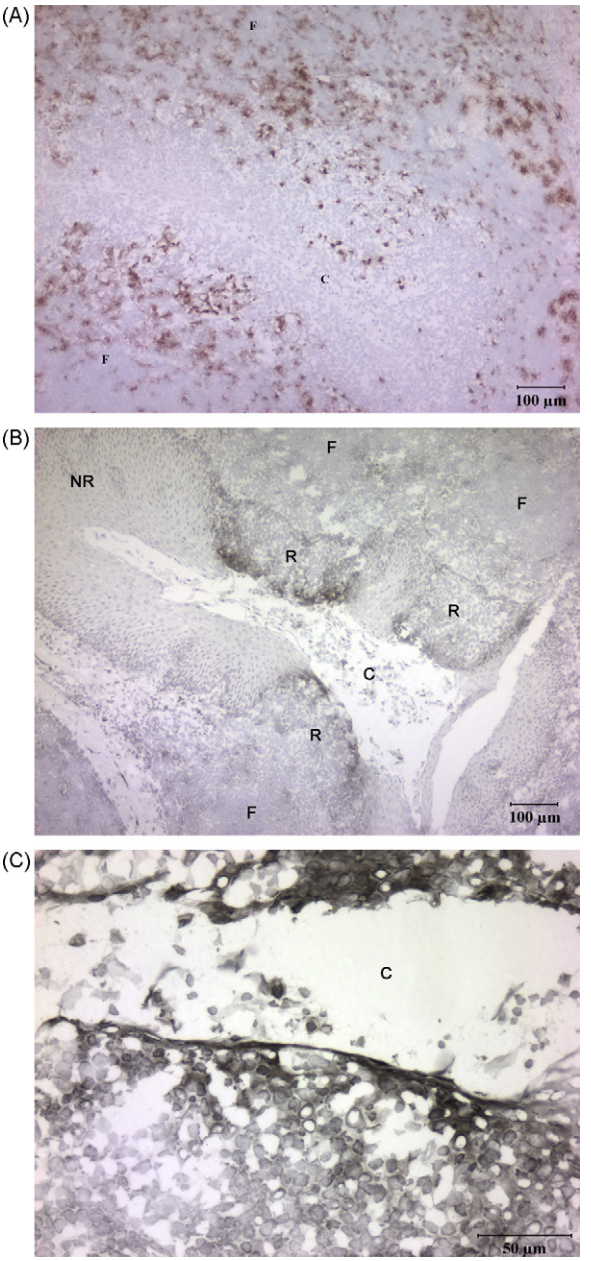

Fig. 8. Section of palatine tonsil from a 7-month-old steer. (A) Labeling for CD68+ cells reveals immunoreactive cells scattered within follicle, interfollicular areas and reticular epithelium. DAB-Ni, Harris hematoxylin counterstain. Bar = 100 μm. (B) In contrast, labeling of CD14+ cells reveals immunoreactive cells limited to reticular epithelium. DAB-Ni, Harris hematoxylin counterstain. Bar = 100 μm. (C) Attenuated, angular cells of the surface layer are densely immunoreactive for the CD14 surface antigen. DAB-Ni, Harris hematoxylin counterstain. Bar = 50 μm. NR: non-reticular epithelium, R: reticular epithelium, F: follicle, C: tonsilar crypt lumen.

in different organs and can vary in different regions of the same organ. Therefore, the presence of microvilli is not sufficient to identify cells as M-cells (Liebler-Tenorio and Pabst, 2006; Paar et al., 1992). Indeed, evidence of endocytosis and antigen transport is required to definitively identify cells as M-cells (Gebert and Pabst, 1999).

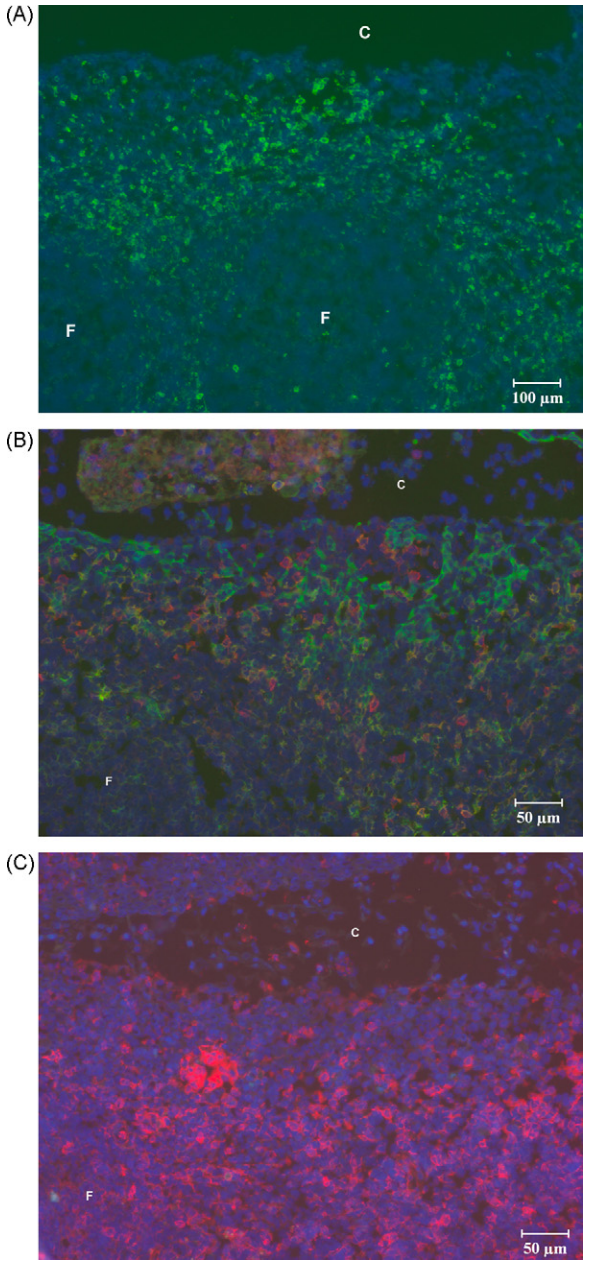

Fig. 9. Section of palatine tonsil from a 7-month-old steer. (A) CD11c+ cells are numerous in interfollicular regions and reticular epithelium. Immunofluorescence. Bar = 100 μm. (B) Both CD11c+ (green) and CD172a+ (red) cells are found in reticular epithelium, CD11c+ cells are more numerous. Some cells stain for both CD11c and CD172a (orange). Immunofluorescence. Bar = 50 μm. (C) Within reticular epithelium, CD172a+ cells are occasionally found in clusters. Immunofluorescence. Bar = 50 μm. (For interpretation of the references to color in this figure legend, the reader is referred to the web version of the article.)

One possible reason M-cells have not been identified in bovine palatine tonsil is the variable morphology of M-cells between different anatomic sites. M-cells in the bovine nasopharyngeal tonsil, with its ciliated pseudostratified columnar epithelium, resemble classic M-cells of ileal dome follicle-associated epithelium. M-cells with similar classic morphology have not been identified in the bovine palatine tonsil with it's associated stratified squamous epithelium. M-cells have been identified in other species in mucosal sites with a stratified squamous epithelium such as conjunctiva (Knop and Knop, 2005; Latkovic, 1989; Liu et al., 2005; Meagher et al., 2005). Light and electron microscopic descriptions of those M-cells are similar to those reported in the present study (Knop and Knop, 2005). M-cells of the rabbit and human palatine tonsil have been shown to form pockets that contain intraepithelial lymphocytes and are separated from the crypt lumen by an attenuated extension of M-cell apical cytoplasm (Gebert, 1997; Howie, 1980), morphologically similar to the arrangement seen in the present findings. The formation of a thin rim of apical cytoplasm separating lymphocytes from the crypt lumen shortens the passage of transcytosed antigen.

Human tonsils have been described as the "Peyer's patches" of the upper respiratory tract (Bernstein et al., 1999), where they serve as a site for antigen uptake and processing leading to the generation of antigen specific T and B cell responses. According to the dogma of the common mucosal immune system, these antigen specific lymphocytes migrate to other mucosal sites or back to the tonsil. Demonstration of bovine palatine tonsilar reticular epithelium with cells morphologically consistent with M-cells of other species, and infiltrated with a population of lymphoid and other mononuclear cells similar to that seen in Peyer's patches, suggests that the bovine palatine tonsil is an important site for antigen uptake and initiation of immune response. A better understanding of palatine tonsilar epithelium will be important in elucidating the pathogenesis of various bovine disease where tonsils plays a critical role as well as aiding in the development of vaccines that could target palatine tonsilar M-cells for efficient vaccine uptake and processing.

Acknowledgements

The authors thank Theresa Anspach, Jason Crabtree, Jay Steffen, Doug Ewing, and Todd Holtz for animal care and Bart Olthoff, Jessica Pollock, Rachel Huegel, Mike Howard, Shelly Zimmerman, Judith Stasko, Michele Fenneman, and Virginia Montgomery for technical assistance. Mention of trade names or commercial products in this article is solely for the purpose of providing specific information and does not imply recommendation or endorsement by the U.S. Department of Agriculture. This project was funded in part by Veterinary Services, Animal and Plant Health Inspection Service, USDA.

References

Ackermann, M.R., DeBey, B.M., Stabel, T.J., Gold, J.H., Register, K.B., Meehan, J.T., 1994. Distribution of anti-CD68 (EBM11) immunoreactivity in formalin-fixed, paraffin-embedded bovine tissues. Vet. Pathol. 31, 340–348.

Barclay, A.N., Brown, M.H., 2006. The SIRP family of receptors and immune regulation. Nat. Rev. 6, 457–464.

Bastos, R.G., Johnson, W.C., Brown, W.C., Goff, W.L., 2007. Differential response of splenic monocytes and DC from cattle to microbial stimulation with *Mycobacterium bovis* BCG and *Babesia bovis* merozoites. Vet. Immunol. Immunopathol. 115, 334–345.

Bernstein, J.M., Gorfien, J., Brandtzaeg, P., 1999. The immunobiology of the tonsils and adenoid. In: Orga, P.L. (Ed.), Mucosal Immunology. Academic Press, San Diego, pp. 1339–1359.

Briggs, R.E., Frank, G.H., Purdy, C.W., Zehr, E.S., Loan, R.W., 1998. Rapid spread of a unique strain of *Pasteurella haemolytica* serotype 1 among transported calves. Am. J. Vet. Res. 59, 401–405.

Brooke, G.P., Parsons, K.R., Howard, C.J., 1998. Cloning of two members of the SIRP alpha family of protein tyrosine phosphatase binding proteins in cattle that are expressed on monocytes and a subpopulation of dendritic cells and which mediate binding to CD4 T cells. Eur. J. Immunol. 28, 1–11.

Cassidy, J.P., Bryson, D.G., Neill, S.D., 1999. Tonsillar lesions in cattle naturally infected with *Mycobacterium bovis*. Vet. Rec. 144, 139–142.

Casteleyn, C., Cornillie, P., Simoens, P., Van Den Broeck, W., 2008. Stereological assessment of the epithelial surface area of the ovine palatine and pharyngeal tonsils. Anat. Histol. Embryol..

Cocquyt, G., Simoens, P., Muylle, S., Van den Broeck, W., 2007. Anatomical and histological aspects of the bovine lingual tonsil. Res. Vet. Sci..

Cocquyt, G., Simoens, P., Muylle, S., Van den Broeck, W., 2008. Anatomical and histological aspects of the bovine lingual tonsil. Res. Vet. Sci. 84, 166–173.

Frink, S., Grummer, B., Pohlenz, J.F., Liebler-Tenorio, E.M., 2002. Changes in distribution and numbers of CD4+ and CD8+ T-lymphocytes in lymphoid tissues and intestinal mucosa in the early phase of experimentally induced early onset mucosal disease in cattle. J. Vet. Med. B: Infect. Dis. Vet. Public Health 49, 476–483.

Gebert, A., 1997. M cells in the rabbit palatine tonsil: the distribution, spatial arrangement and membrane subdomains as defined by confocal lectin histochemistry. Anat. Embryol. 195, 353–358.

Gebert, A., Pabst, R., 1999. M cells at locations outside the gut. Semin. Immunol. 11, 165–170.

Griffin, J.F., Rodgers, C.R., Liggett, S., Mackintosh, C.G., 2006. Tuberculosis in ruminants: characteristics of intra-tonsilar *Mycobacterium bovis* infection models in cattle and deer. Tuberculosis (Edinb) 86, 404–418.

Hein, W.R., Mackay, C.R., 1991. Prominence of gamma delta T cells in the ruminant immune system. Immunol. Today 12, 30–34.

Howie, A.J., 1980. Scanning and transmission electron microscopy on the epithelium of human palatine tonsils. J. Pathol. 130, 91–98.

Knop, N., Knop, E., 2005. Ultrastructural anatomy of CALT follicles in the rabbit reveals characteristics of M-cells, germinal centres and high endothelial venules. J. Anat. 207, 409–426.

Kunkle, R.A., Steadham, E.M., Cheville, N.F., 1995. Morphometric analysis of CD4+, CD8+, and gamma/delta+ T-lymphocytes in lymph nodes of cattle vaccinated with *Brucella abortus* strains RB51 and 19. Vet. Immunol. Immunopathol. 49, 271–279.

Latkovic, S., 1989. Ultrastructure of M-cells in the conjunctival epithelium fo the guinea pig. Curr. Eye Res. 8, 751–755.

Liebler-Tenorio, E.M., Greiser-Wilke, I., Pohlenz, J.F., 1997. Organ and tissue distribution of the antigen of the cytopathogenic bovine virus diarrhea virus in the early and advanced phase of experimental mucosal disease. Arch. Virol. 142, 1613–1634.

Liebler-Tenorio, E.M., Pabst, R., 2006. MALT structure and function in farm animals. Vet. Res. 37, 257–280.

Liu, H., Meagher, C.K., Moore, C.P., Phillips, T.E., 2005. M cells in the follicle-associated epithelium of the rabbit conjunctiva preferentially bind and translocate latex beads. Invest. Ophthalmol. Vis. Sci. 46, 4217–4223.

Liu, Y., Buhring, H.J., Zen, K., Burst, S.L., Schnell, F.J., Williams, I.R., Parkos, C.A., 2002. Signal regulatory protein (SIRPalpha), a cellular ligand for CD47, regulates neutrophil transmigration. J. Biol. Chem. 277, 10028–10036.

Lugton, I., 1999. Mucosa-associated lymphoid tissues as sites for uptake, carriage and excretion of tubercle bacilli and other pathogenic mycobacteria. Immunol. Cell. Biol. 77, 364–372.

Manesse, M., Delverdier, M., Abella-Bourges, N., Sautet, J., Cabanie, P., Schelcher, F., 1998. An immunohistochemical study of bovine palatine and pharyngeal tonsils at 21. 60 and 300 days of age. Anat. Histol. Embryol. 27, 179–185.

Meagher, C.K., Liu, H., Moore, C.P., Phillips, T.E., 2005. Conjunctival M cells selectively bind and translocate Maackia amurensis leukoagglutinin. Exp. Eye Res. 80, 545–553.

Miyazawa, K., Aso, H., Honda, M., Kido, T., Minashima, T., Kanaya, T., Watanabe, K., Ohwada, S., Rose, M.T., Yamaguchi, T., 2006. Identification of bovine dendritic cell phenotype from bovine peripheral blood. Res. Vet. Sci. 81, 40–45.

Nickel, R.A., Schummer, E., Seiferle, E., 1979. The viscera of domestic animals. Verlag Paul Parley, Berlin, pp. 52–56.

Paar, M., Liebler, E.M., Pohlenz, J.F., 1992. Uptake of ferritin by follicle-associated epithelium in the colon of calves. Vet. Pathol. 29, 120–128.

Palmer, M.V., Whipple, D.L., Olsen, S.C., 1999a. Development of a model of natural infection with *Mycobacterium bovis* in white-tailed deer. J. Wildl. Dis. 35, 450–457.

Palmer, M.V., Whipple, D.L., Rhyan, J.C., Bolin, C.A., Saari, D.A., 1999b. Granuloma development in cattle after intratonsilar inoculation with *Mycobacterium bovis*. Am. J. Vet. Res. 60, 310–315.

Perry, M., Whyte, A., 1998. Immunology of the tonsils. Immunol. Today 19, 414–421.

Perry, M.E., 1994. The specialized structure of crypt epithelium in the human palatine tonsil and its functional significance. J. Anat. 185, 111–127.

Press, C., McClure, S., Landsverk, T., 1991. Computer-assisted morphometric analysis of absorptive and follicle-associated epithelia of Peyer's patches in sheep foetuses and lambs indicates the presence of distinct T- and B-cell components. Immunology 72, 386–392.

Pugin, J., Heumann, I.D., Tomasz, A., Kravchenko, V.V., Akamatsu, Y., Nishijima, M., Glauser, M.P., Tobias, P.S., Ulevitch, R.J., 1994. CD14 is a pattern recognition receptor. Immunity 1, 509–516.

Rebelatto, M.C., Mead, C., HogenEsch, H., 2000. Lymphocyte populations and adhesion molecule expression in bovine tonsils. Vet. Immunol. Immunopathol. 73, 15–29.

Renjifo, X., Howard, C., Kerkhofs, P., Denis, M., Urbain, J., Moser, M., Pastoret, P.P., 1997. Purification and characterization of bovine dendritic cells from peripheral blood. Vet. Immunol. Immunopathol. 60, 77–88.

Schuh, J.C., Oliphant, L.W., 1992. Development and immunophenotyping of the pharyngeal tonsil (adenoid) in cattle. J. Comp. Pathol. 106, 229–241.

van Beek, E.M., Cochrane, F., Barclay, A.N., van den Berg, T.K., 2005. Signal regulatory proteins in the immune system. J. Immunol. 175, 7781–7787.

Velinova, M., Thielen, C., Melot, F., Donga, J., Eicher, S., Heinen, E., Antoine, N., 2001. New histochemical and ultrastructural observations on normal bovine tonsils. Vet. Rec. 149, 613–617.

Vignery, A., 2005. Macrophage fusion: are somatic and cancer cells possible partners? Trends Cell Biol. 15, 188–193.

Wells, G.A.H., Spiropoulos, J., Hawkins, S.A.C., Ryder, S.J., 2005. Pathogenesis of experimental bovine spongiform encephalopathy: preclinical infectivity in tonsil and observations on the distribution of lingual tonsil in slaughtered cattle. Vet. Rec. 156, 401–407.

Zen, K., Parkos, C.A., 2003. Leukocyte–epithelial interactions. Curr. Opin. Cell Biol. 15, 557–564.